

Viscosity, Interfacial Tension, Self-Diffusion Coefficient, Density, and Refractive Index of the Ionic Liquid 1-Ethyl-3-methylimidazolium Tetracyanoborate as a Function of Temperature at Atmospheric Pressure

Thomas Koller,[†] Michael H. Rausch,^{†,‡} Peter S. Schulz,[§] Markus Berger,[§] Peter Wasserscheid,[§] Ioannis G. Economou,^{||} Alfred Leipertz,^{†,‡} and Andreas P. Fröba^{*,†,‡}

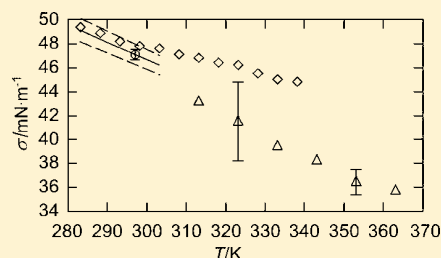
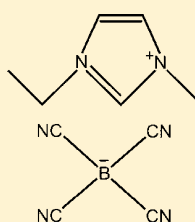
[†]Erlangen Graduate School in Advanced Optical Technologies (SAOT), University of Erlangen-Nuremberg, Paul-Gordan-Straße 6, D-91052 Erlangen, Germany

[‡]Institute of Engineering Thermodynamics (LTT), University of Erlangen-Nuremberg, Am Weichselgarten 8, D-91058 Erlangen, Germany

[§]Institute of Chemical Reaction Engineering (CRT), University of Erlangen-Nuremberg, Egerlandstraße 3, D-91058 Erlangen, Germany

^{||}Department of Chemical Engineering, The Petroleum Institute (PI), PO Box 2533, Abu Dhabi, United Arab Emirates

ABSTRACT: Thermophysical properties of the ionic liquid (IL) [EMIM][B(CN)₄] (1-ethyl-3-methylimidazolium tetracyanoborate) were investigated both by conventional techniques and by surface light scattering (SLS) at atmospheric pressure. The density was measured between (283.15 and 363.15) K with a vibrating U-tube densimeter. An Abbe refractometer was used for the measurement of the refractive index in the range from (283.15 to 313.15) K. Self-diffusion coefficients for the cation and anion were measured by nuclear magnetic resonance (NMR) spectroscopy from (273.15 to 318.15) K. The interfacial tension was obtained from the pendant drop technique at 297.04 K. Based on this datum and the temperature dependence of density, the interfacial tension for all relevant temperatures was estimated via an appropriate prediction model. For the IL studied within the present work, the quantity directly accessible by SLS at low temperatures was the ratio of dynamic viscosity to interfacial tension. Combining the results from SLS with the density and interfacial tension data obtained from conventional methods, the dynamic viscosity could be determined from (283.15 to 303.15) K. For higher temperatures, SLS measurements combined with the results for density allowed the simultaneous determination of dynamic viscosity and interfacial tension from (313.15 to 363.15) K. Besides a comparison with literature data for [EMIM][B(CN)₄], the influence of variation of the anion in [EMIM]-based ILs on thermophysical properties is discussed. It could be shown that the thermophysical properties of [EMIM][B(CN)₄] are mainly affected by the distinct charge delocalization in the anion.



INTRODUCTION

In the past decade, ionic liquids (ILs) have generated a lot of interest for chemistry and chemical engineering.¹ Due to an almost unlimited number of potential combinations of cations and anions,² these salts which are in a liquid state below 100 °C can be tailored to specific applications in many fields of technology.^{3–9} The variety of possible ILs, however, is the reason that the experimental determination of a complete set of their thermophysical properties is virtually impossible, since it would cause an enormous investment in time and resources.¹⁰

The IL [EMIM][B(CN)₄] (1-ethyl-3-methylimidazolium tetracyanoborate) investigated in the present work has been selected for our detailed study due to its high potential for electrolyte applications, for example, in dye-sensitized solar cells. [EMIM][B(CN)₄] provides a unique combination of highly interesting properties for these applications such as a wide

electrochemical window, very low viscosity, hydrophobicity, and hydrolytic stability.^{11,12} Furthermore, [EMIM][B(CN)₄] is considered to be a very promising extraction solvent and separation reagent. Mahurin et al.¹³ found that [EMIM][B(CN)₄], which possesses four nitrile groups in the anion, shows the highest separation selectivity for CO₂/N₂ and the highest solubility for CO₂ compared to ILs based on the [BMIM]⁺ (1-butyl-3-methylimidazolium) cation combined with anions carrying a lower number of nitrile groups, for example, [N(CN)₂][–] (dicyanamide) or [C(CN)₃][–] (tricyanomethanide), and even in comparison with the popular IL [EMIM][NTf₂] (1-ethyl-3-methylimidazolium bis(trifluoromethylsulfonyl)imide).

Received: October 7, 2011

Accepted: February 1, 2012

Published: February 17, 2012

Ravichandar et al.¹⁴ underlined the high solubility of CO₂ in [EMIM][B(CN)₄] with molecular simulations. A literature survey, however, reveals that only a limited number of thermophysical and especially transport properties required for process and apparatus design are available for [EMIM][B(CN)₄].^{13,15–18}

In former works,^{19,20} we have shown that surface light scattering (SLS) can provide reliable viscosity data for ILs. For various imidazolium-based ILs differing in the cation and anion, the viscosity was measured over a temperature range from (273 to 333) K at atmospheric pressure. The estimated expanded uncertainty with a level of confidence of approximately 95 % ($k = 2$) was less than 3 %. In comparison to conventional techniques, the main advantage of the SLS technique is the possibility of determining the viscosity and, in some cases, also the interfacial tension in macroscopic thermodynamic equilibrium in an absolute way without the need of any calibration procedure.^{21,22}

The present work provides reliable dynamic viscosity, interfacial tension, self-diffusion coefficient, and density as well as refractive index data for [EMIM][B(CN)₄] in dependence on temperature at atmospheric pressure by SLS and conventional techniques. Compared with the ILs investigated previously^{19,20,23} as well as literature data for other ILs, the influence of varying anions on the thermophysical properties of [EMIM]-based ILs is pointed out.

■ EXPERIMENTAL SECTION

Material and Sample Preparation Procedure. [EMIM]-[B(CN)₄] (molecular weight $M = 226.05 \text{ g}\cdot\text{mol}^{-1}$) was purchased from Merck KGaA, Germany, with a nominal purity higher than 98 %. The purity of [EMIM][B(CN)₄] was proved by ¹H NMR analysis (JEOL, ECX +400 spectrometer), where dimethylsulfoxide-*d*₆ (DMSO-*d*₆) was used as solvent. The total peak integral in the ¹H NMR spectrum was found to correspond to a nominal purity even higher than 99 %. Before use, the IL was dried at about 333.15 K for a period of at least 4 h on a vacuum line (0.5 mbar) with an oil-sealed vacuum pump and a liquid nitrogen trap. The concentration of water by mass was proved twice by Karl Fischer coulometric titration (Metrohm, 756 KF coulometer) after the SLS experiments. The expanded uncertainty ($k = 2$) of these measurements yielding values of (730 and 700) ppm is estimated to be less than ± 20 %. The transfer of samples was performed under an argon atmosphere. All parts of the measuring devices which were in contact with the sample as well as all glassware used for sample handling were cleaned with ethanol, rinsed with deionized water, and oven-dried.

Vibrating Tube Method: Density. Density measurements at atmospheric pressure are based on the vibrating-tube method. For the density meter (Anton Paar, DMA 5000) used here, long-term drift is eliminated by a reference oscillator built into the measuring cell. Only one adjustment at 293.15 K is sufficient to reach a high accuracy for the whole measuring temperature range. The DMA 5000 allows a full-range viscosity correction, whereby all viscosity related errors inherent to all known types of oscillating U-tube density meters are automatically eliminated. The temperature of the U-tube is controlled within ± 1 mK and measured by a high-precision platinum resistance probe with an absolute uncertainty of ± 10 mK. For the density meter calibration, standard water and air were used. The expanded uncertainty ($k = 2$) of the present density measurements for the IL is estimated to be less than ± 0.02 %. For this, the calibration error of the apparatus of 0.01 %

and the error associated with the measurement procedure for the IL have been taken into account. The precision or repeatability of the instrument was better than ± 0.001 %.

Abbe Refractometer: Refractive Index. The refractive index n_D at the sodium line ($\lambda_D = 589.3 \text{ nm}$) and the refractive index difference $n_F - n_C$ for the Fraunhofer lines F ($\lambda_F = 486.1 \text{ nm}$) and C ($\lambda_C = 656.3 \text{ nm}$) were measured with an Abbe refractometer (Leo Kuebler, R 6000 G). The temperature of the samples was controlled with a laboratory thermostat within ± 0.02 K and measured by a mercury thermometer with an absolute uncertainty of ± 0.5 K. The refractometer was calibrated with water. Its expanded uncertainties ($k = 2$) in the measurement of the refractive index and the refractive index difference are estimated to be less than ± 0.0005 and ± 0.001 .

NMR Spectroscopy: Self-Diffusion Coefficient. The self-diffusion coefficients D of the [EMIM]⁺ cation and [B(CN)₄]⁻ anion were derived from NMR experiments. The pulsed-field gradient spin-echo NMR measurements were performed by using ¹H nuclei in the methyl and ethyl chain of the cation and ¹¹B nucleus of the anion. A bipolar pulse longitudinal eddy current delay was applied as pulse sequence with a sine gradient shape. In this case, the Stejskal-Tanner equation has to be modified according to Price,²⁴

$$I = I_0 \exp\left(-D \cdot \gamma^2 \delta^2 G^2 \left(\frac{4\Delta - \delta}{\pi^2}\right)\right) \quad (1)$$

where I and I_0 are the intensities of a resonance in the presence and in the absence of the pulsed-field gradient G , γ is the gyromagnetic ratio ($2.675 \cdot 10^{-8} \text{ rad}\cdot\text{T}^{-1}\cdot\text{s}^{-1}$ for ¹H and $0.8585 \cdot 10^{-8} \text{ rad}\cdot\text{T}^{-1}\cdot\text{s}^{-1}$ for ¹¹B), δ is the duration of the pulsed-field gradient, and Δ is the time between the two gradient pulses. Plotting $\log(I \cdot I_0^{-1})$ versus G^2 , a straight line was obtained whose slope is directly proportional to D . A Shigemi tube matched with deuterated chloroform (CDCl₃) was used to prevent convection within the sample. The temperature stability during the experiments was better than ± 0.5 K, and the absolute uncertainty in the temperature measurement was ± 0.05 K. The expanded uncertainty ($k = 2$) of the NMR experimental data was estimated to be less than ± 10 %.

Pendant Drop Technique: Interfacial Tension. For the evaluation of the dynamic viscosity from SLS, interfacial tension data are needed in the case of an overdamped behavior of surface fluctuations. For an accurate determination of the dynamic viscosity, it has to be ensured that the liquid surface conditions for the pendant drop technique providing interfacial tension data are equal to those for the SLS measurements. This was ensured by investigating identical samples of the IL by both methods. Here, a universal surface analyzer (OEG, SURFTENS universal) was used, where the geometrical profile of a pendant drop is compared with the theoretical drop profile obtained from the Laplace equation. The measurements were performed inside an optical glass cell for photometry (Hellma, 402.000) at well-defined conditions for a temperature of $(297.04 \pm 0.1) \text{ K}$. For the interfacial tension data of the IL, the expanded uncertainty ($k = 2$) was estimated to be less than ± 1 %.

Surface Light Scattering (SLS): Viscosity and Interfacial Tension. For a detailed description of the fundamentals and methodological principles of SLS, the reader is referred to specialized literature.^{21,25–28} Here, a more specific treatment of the theory of SLS was used by inspecting the hydrodynamic capillary wave problem in the limiting case of a free liquid surface, neglecting the presence of a second fluid phase. For the

present investigations of a phase boundary between an IL and argon at atmospheric pressure, this can be carried out without any significant loss of accuracy because the vapor properties are very small compared to the respective liquid quantities.^{19,20} In this case, the decay dependence on time t of a particular surface mode of the form $\exp[i\vec{q}\vec{r} + i\alpha t]$, with a wave vector \vec{q} at a given point \vec{r} , is obtained from the dispersion equation²⁷

$$\left(i\alpha + \frac{2\eta q^2}{\rho} \right)^2 + \frac{\sigma q^3}{\rho} + gq - \frac{4\eta^2 q^4}{\rho^2} \sqrt{1 + \frac{i\alpha\rho}{\eta q^2}} = 0 \quad (2)$$

where g is the acceleration of gravity and η , σ , and ρ are the dynamic viscosity, interfacial tension, and density of the liquid, respectively. Data for the dynamic viscosity and in addition for a limited temperature range for the interfacial tension of the IL were obtained by an exact numerical solution of the dispersion equation, eq 2. Here, two physical solutions for the temporal decay of surface fluctuations and thus for the complex frequency α have to be considered. For temperatures between (313.15 and 363.15) K, surface fluctuations showed an oscillatory behavior corresponding to the complex frequency $\alpha_{1,2} = \pm \omega_q + i\Gamma_{1,2}$. Here, the real part represents the frequency ω_q and the imaginary part the damping Γ of the surface mode observed. The decay time of the fluctuations $\tau_C = \Gamma^{-1}$ as well as the frequency of their propagation ω_q could be used to determine η and σ simultaneously. For temperatures between (283.15 and 303.15) K, surface fluctuations were overdamped and did not propagate ($\omega_q = 0$). In this case, the complex frequency is associated with two different damping rates $\alpha_{1,2} = i\Gamma_{1,2}$. For the IL [EMIM][B(CN)₄] investigated here, from the two modes decaying at different rates only the one associated with α_1 could be resolved. By this, besides the decay time $\tau_{C,1}$ of surface fluctuations at a given wave number q determined in the experiment, interfacial tension data from the pendant drop method were used for an exact evaluation of the dynamic viscosity. In addition, the densities ρ measured by the oscillating U-tube densimeter were used for analysis of the SLS data in both cases.

The expanded uncertainty ($k = 2$) for the dynamic viscosity η in the overdamped regime is estimated to be less than $\pm 3\%$. In the transition regime between an overdamped and an oscillatory behavior for the temperature range from (313.15 to 333.15) K, the expanded uncertainties ($k = 2$) for the dynamic viscosity are estimated to be less than $\pm 6\%$ and for the interfacial tension σ less than $\pm 8\%$. The reason for the relatively large uncertainties is caused by the experimental complexity in the transition regime. For higher temperatures from (343.15 to 363.15) K, the expanded uncertainties ($k = 2$) regarding η and σ are estimated to be less than $\pm 3\%$. The experimental setup used for the investigation of [EMIM][B(CN)₄] is the same as that employed in our former SLS investigations for different ILs^{19,20} and includes a laser (Coherent, Verdi-2 V; laser wavelength in vacuo $\lambda_0 = 532$ nm; operated at 500 mW), correlator (ALV-7004), optical and electro-optical parts, sample cell (aluminum; inner diameter, 70 mm; volume, 150 cm³), and thermostat. Scattered light is detected in the forward direction near refraction perpendicular to the surface plane at variable and relatively high wave numbers. For this arrangement, the modulus of the wave vector, $q = (2\pi/\lambda_0)\sin(\Theta_E)$, of the observed surface vibration mode can be deduced as a function of the easily accessible angle of incidence Θ_E .

For the experiment, the angle of incidence Θ_E was set between 3.0° and 3.2° and measured with a high precision rotation table with an uncertainty of $\pm 0.005^\circ$. The temperature of the cell was measured with two calibrated 100 Ω platinum resistance probes integrated into the main body of the vessel, with a resolution of 0.25 mK, using an ac bridge (Anton Paar, MKT 100). The uncertainty of the absolute temperature measurement was less than ± 15 mK. The temperature stability during an experimental run was better than ± 2 mK. For each temperature, six measurements at different angles of incidence were performed.

RESULTS AND DISCUSSION

In the following, the results for density, refractive index, self-diffusion coefficients, interfacial tension, and dynamic viscosity are discussed in subsequences. First, the obtained data will be interpreted in connection with the intermolecular interactions by comparison with previously investigated [EMIM]-based ILs. Thereafter, the respective thermophysical properties are compared to available literature. In general, a lack of literature data for the IL investigated in this work can be found.

Density. The experimental density data obtained for temperatures between (283.15 and 363.15) K at atmospheric pressure are summarized in Table 1. The densities for

Table 1. Density ρ of [EMIM][B(CN)₄] from $T = (283.15$ to $363.15)$ K at Atmospheric Pressure

T	ρ
K	g·cm ⁻³
283.15	1.04833
288.15	1.04431
293.15	1.04031
298.15	1.03634
303.15	1.03240
308.15	1.02848
313.15	1.02459
318.15	1.02072
323.15	1.01687
328.15	1.01306
333.15	1.00926
338.15	1.00549
343.15	1.00174
348.15	0.99801
353.15	0.99428
358.15	0.99059
363.15	0.98692

[EMIM][B(CN)₄] ρ_{calc} can be represented by a polynomial of second order with respect to temperature T in K,

$$\rho_{\text{calc}} = \rho_0 + \rho_1 T + \rho_2 T^2 \quad (3)$$

where all data have been taken into account with the same statistical weight. The fit parameters in eq 3 for the IL studied were determined to be $\rho_0 = 1.31360$ g·cm⁻³, $\rho_1 = -1.06920 \cdot 10^{-3}$ g·cm⁻³·K⁻¹, and $\rho_2 = 4.67194 \cdot 10^{-7}$ g·cm⁻³·K⁻². The root-mean-square deviation of the experimental density data from the correlation according to eq 3 is 0.0014 %, while the relative deviation of all single data points from the fit lies clearly within the measurement uncertainty of $\pm 0.02\%$. Fredlake and co-workers²⁹ report that for ILs with anions that are small enough to easily occupy close-approach positions

around the relatively large cation an increasing molar weight of the anion causes an increase of density. For most of the [EMIM]-based ILs investigated in previous works,^{19,20,23} the density increases with increasing molecular weight of the respective anions. Only for the two ILs [EMIM][MeSO₃] and [EMIM][O₂CSO₄], the densities do not match this behavior. The present experimental results reveal that [EMIM][B(CN)₄] has the lowest density compared with the previously studied [EMIM]-based ILs.^{19,20,23} For instance, its density is distinctly lower than that of [EMIM][N(CN)₂],¹⁹ for example, $\Delta\rho = -6.3\%$ at 283.15 K and -7.5% at 363.15 K based on the [EMIM][N(CN)₂] densities, although [B(CN)₄]⁻ has a higher molecular weight than [N(CN)₂]⁻. This might be explained by the larger volume of the tetrahedral [B(CN)₄]⁻ anion with four cyano groups disturbing the formation of molecular assemblies. In addition, the strong charge delocalization¹¹ and thus relatively weak coordination³⁰ of [B(CN)₄]⁻ to [EMIM]⁺ seems to result in a small density. The same influences appear to be the reasons for the lower density of [EMIM][B(CN)₄] compared to [EMIM][BF₄]²³ possessing also an anion of lower molecular weight. The distinctly larger density of [EMIM][NTf₂]¹⁹ compared with [EMIM][B(CN)₄] is in agreement with the conclusions of Fredlake et al.²⁹ due to the high molecular weight of [NTf₂]⁻.

The deviations between the correlation developed from our experimental results, eq 3, and literature data are shown in Figure 1. Tong et al.¹⁶ measured the density of [EMIM][B(CN)₄]

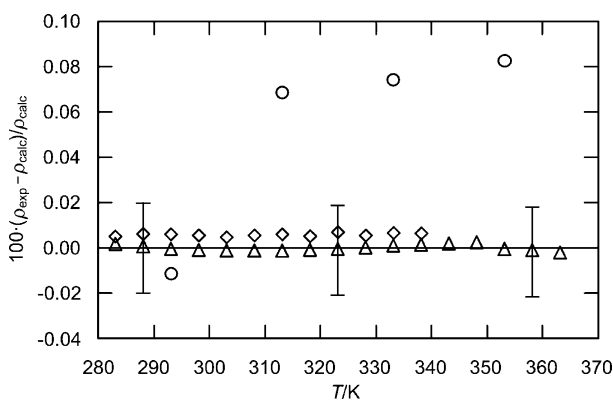


Figure 1. Deviation of experimental liquid densities ρ of [EMIM][B(CN)₄] at atmospheric pressure for temperatures between (283.15 and 363.15) K from the correlation (—, eq 3): Δ , this work; \diamond , Tong et al.;¹⁶ \circ , Uerdingen.¹⁷ Estimated expanded uncertainties ($k = 2$) of the present measurements are exemplarily shown as error bars.

for temperatures from (283.15 to 338.15) K with an Anton Paar DMA 4500 oscillating U-tube densimeter, providing automatic viscosity correction. The given uncertainty of $\pm 0.00001 \text{ g}\cdot\text{cm}^{-3}$ seems to be underestimated, that is, below the expected value when taking into account both the error associated with the calibration and that of the subsequent measuring procedure. However, their data show relatively good agreement with our results as the deviation of their single data points are less than 0.01 % from the correlation obtained in this work. The measurements provided by Uerdingen¹⁷ using an Anton Paar SVM 3000 viscosimeter show larger deviations from our fit, for example, from -0.01% at 293.15 K up to 0.08% at 353.15 K. The experimental uncertainties are specified to be $\pm 0.0005 \text{ g}\cdot\text{cm}^{-3}$. The datum of Mahurin et al.¹³ at 298 K, which is not shown in Figure 1, strongly deviates by -0.62%

with respect to our correlation, eq 3. Neither method nor uncertainty are stated in the work of Mahurin et al.¹³

Refractive Index. The measured data for the refractive index n_D and the refractive index difference $n_F - n_C$ for the IL [EMIM][B(CN)₄] in the temperature range from (283.15 to 313.15) K at atmospheric pressure are summarized in Table 2.

Table 2. Refractive Index n_D and Refractive Index Difference $n_F - n_C$ of [EMIM][B(CN)₄] from $T = (283.15 \text{ to } 313.15)$ K at Atmospheric Pressure

T/K	n_D	$n_F - n_C$
283.15	1.4533	0.0099
293.15	1.4499	0.0098
303.15	1.4465	0.0095
313.15	1.4432	0.0094

The refractive index n_{calc} can be calculated by the linear equation

$$n_{\text{calc}} = n_0 + n_1 T + \frac{\Delta n}{\Delta \lambda} (\lambda - \lambda_D) \quad (4)$$

where T represents the temperature in K, λ the wavelength in m, and $\lambda_D (= 589.3 \cdot 10^{-9} \text{ m})$ the wavelength of the sodium vapor line. In eq 4, the fit parameters considering the present results are $n_0 = 1.54870$ and $n_1 = -0.000337 \text{ K}^{-1}$, and the mean dispersion is $\Delta n / \Delta \lambda = -56776 \text{ m}^{-1}$. The latter corresponds to the average value of the refractive index differences $n_F - n_C$ and is assumed to be independent of temperature. For [EMIM][B(CN)₄], the root-mean-square deviation of the experimental refractive index data n_D from their correlation according to eq 4 is 0.004 %. The deviations of the single data points from the fit are clearly within the measurement uncertainty of ± 0.0005 . Deetlefs et al.³¹ and Brocos et al.³² report that the larger the reduced molar free volume is, that is, the unoccupied part of the molar volume of a substance, the smaller is its refractive index. This is in good agreement with the behavior of the refractive indices of the [EMIM]-based ILs investigated in previous works.^{19,20} A comparison with these ILs reveals that [EMIM][B(CN)₄] possesses a relatively small refractive index. For instance, [EMIM][B(CN)₄] shows a smaller refractive index than [EMIM][N(CN)₂]¹⁹ which can be explained by its lower density in consequence of the high charge delocalization and large volume of [B(CN)₄]⁻. The smaller refractive index of [EMIM][NTf₂]¹⁹ with respect to [EMIM][B(CN)₄] is probably due to the distinctly larger volume of the anion, resulting in larger reduced molar free volume and less refraction.

Self-Diffusion Coefficient. The self-diffusion coefficients of the cation D_+ and of the anion D_- in the temperature range from (273.15 to 318.15) K at atmospheric pressure are summarized in Table 3 and Figure 2. The self-diffusion coefficients in dependence on temperature T in K follow an Arrhenius behavior for the limited temperature range,

$$D_{+/-} = D_{0,+/-} \exp\left(-\frac{E_{A,+/-}}{RT}\right) \quad (5)$$

with the pre-exponential factor D_0 and the activation energy for the self-diffusion E_A of the cation (+) and of the anion (-), respectively. For [EMIM][B(CN)₄], the corresponding values determined by the fit of eq 5 are $D_{0,+} = 8.66 \cdot 10^{-6} \text{ m}^2 \cdot \text{s}^{-1}$ and $D_{0,-} = 3.14 \cdot 10^{-6} \text{ m}^2 \cdot \text{s}^{-1}$, as well as $E_{A,+} = 29.45 \text{ kJ}\cdot\text{mol}^{-1}$ and

Table 3. Self-Diffusion Coefficients of the Cation $[\text{EMIM}]^+$ (D_+) and of the Anion $[\text{B}(\text{CN})_4]^-$ (D_-) from $T = (273.15$ to $318.15)$ K at Atmospheric Pressure

T K	$10^{12} D_+$ $\text{m}^2\cdot\text{s}^{-1}$	$10^{12} D_-$ $\text{m}^2\cdot\text{s}^{-1}$
273.15	19.8	25.0
283.15	31.9	38.5
288.15	41.5	40.6
293.15	50.7	48.8
298.15	58.1	69.3
308.15	86.1	97.8
318.15	128.0	125.5

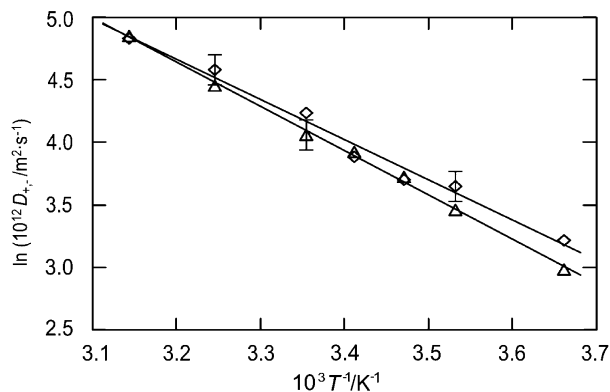


Figure 2. Self-diffusion coefficients of the cation $[\text{EMIM}]^+$ (D_+) and of the anion $[\text{B}(\text{CN})_4]^-$ (D_-) in $[\text{EMIM}][\text{B}(\text{CN})_4]$ at atmospheric pressure as a function of temperature: Δ , $[\text{EMIM}]^+$; \diamond , $[\text{B}(\text{CN})_4]^-$. Lines are based on the fit according to eq 5. Estimated expanded uncertainties ($k = 2$) of the present measurements are exemplarily shown as error bars.

$E_{A,+} = 26.74 \text{ kJ}\cdot\text{mol}^{-1}$. In eq 5, R ($= 8.3145 \text{ J}\cdot\text{mol}^{-1}\cdot\text{K}^{-1}$) represents the universal gas constant.

Since there are no literature data available for $[\text{EMIM}][\text{B}(\text{CN})_4]$ as well as different $[\text{B}(\text{CN})_4]$ -based ILs, the self-diffusion coefficients determined in this work can only be compared with other ILs containing the $[\text{EMIM}]^+$ cation to investigate the anion effect. The comparison shows that $[\text{EMIM}][\text{B}(\text{CN})_4]$ exhibits high values for the self-diffusion coefficients. For example, values for $[\text{EMIM}][\text{NTf}_2]$ ($D_+ = 49.5\cdot 10^{-12} \text{ m}^2\cdot\text{s}^{-1}$ and $D_- = 30.9\cdot 10^{-12} \text{ m}^2\cdot\text{s}^{-1}$) at 298 K are lower.³³ A reason for this might be that $[\text{NTf}_2]^-$ is larger than $[\text{B}(\text{CN})_4]^-$, resulting in slower diffusion, in particular of the anion. Correspondingly, the diffusivity of the $[\text{EMIM}]^+$ cation in $[\text{EMIM}][\text{NTf}_2]$ is also reduced. In addition, the comparatively weak interaction between $[\text{B}(\text{CN})_4]^-$ and $[\text{EMIM}]^+$ seems to enhance the self-diffusivity of both ions. Even $[\text{EMIM}][\text{BF}_4]$, which has a smaller but geometrically similar anion compared with $[\text{EMIM}][\text{B}(\text{CN})_4]$, shows lower diffusion coefficients,³⁴ confirming the major contribution of the weak intermolecular interactions in $[\text{EMIM}][\text{B}(\text{CN})_4]$ on the self-diffusion coefficients.

Interfacial Tension. Table 4 and Figure 3 summarize the values obtained for the interfacial tension of $[\text{EMIM}][\text{B}(\text{CN})_4]$ within this work. For temperatures of (313.15 to 363.15) K, interfacial tension was determined from SLS experiments. In addition, one single datum was measured with the pendant drop technique at a temperature of 297.04 K at atmospheric pressure. This value is combined with the temperature dependence of the density to predict the interfacial tension in the

Table 4. Interfacial Tension σ of $[\text{EMIM}][\text{B}(\text{CN})_4]$, Obtained from Pendant Drop Technique at $T = 297.04$ K, and from SLS Experiments in the Range $T = (313.15$ to $363.15)$ K at Atmospheric Pressure

T K	σ $\text{mN}\cdot\text{m}^{-1}$
297.04	47.09
313.15	43.29
323.15	41.60
333.15	39.53
343.15	38.33
353.15	36.52
363.15	35.80

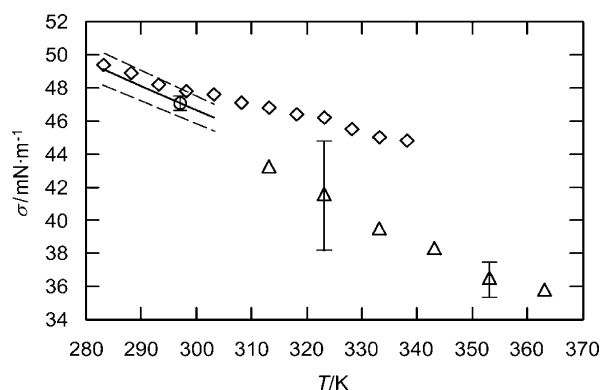


Figure 3. Interfacial tension σ of $[\text{EMIM}][\text{B}(\text{CN})_4]$ at atmospheric pressure as a function of temperature: Δ , this work obtained from pendant drop; \circ , this work obtained from SLS; \diamond , eq 6 using data from pendant drop and density, eq 3; $-$, estimated uncertainty of the prediction, eq 6; \diamond , Tong et al.¹⁶ Estimated expanded uncertainties ($k = 2$) of the present measurements are exemplarily shown as error bars.

temperature range from (283.15 to 303.15) K and to evaluate the dynamic viscosity from the SLS experiments in the same temperature range. The prediction method is based on the MacLeod–Sudgen correlation.³⁵ MacLeod³⁶ suggested a relation between the interfacial tension σ , the liquid density ρ_l , and the vapor density ρ_v , $\sigma^{1/4} = C(\rho_l - \rho_v)$, where C is a constant. Sugden³⁷ modified MacLeod's expression and introduced a temperature-independent parameter, the parachor $P = CM$, which can be estimated from the structure of the molecule. For ILs, the existence of a vapor phase inside the measurement cell can be neglected. Thus, for the prediction of the temperature dependency of interfacial tension, only a single experimental value for the interfacial tension at an arbitrary reference temperature and the knowledge of the temperature dependency of the density are required. The interfacial tension σ at any temperature in this work was predicted by

$$\sigma = \sigma_{\text{ref}}(\rho/\rho_{\text{ref}})^4 \quad (6)$$

where σ_{ref} and ρ_{ref} are the measured interfacial tension and density at the reference temperature 297.04 K. The proposed prediction scheme typically represents the interfacial tension of high viscosity fluids with an uncertainty of less than 2 %, which was tested for several reference fluids, see, for example, ref 22. As expected, the surface tension decreases with increasing temperature; see Figure 3. The experimental SLS values follow an almost linear dependency with respect to T . The predicted values according to eq 6 and the SLS data seem to converge for

low temperatures. Thus, the prediction should be applicable within 2 % over a limited temperature range. Until now, only a limited number of studies on the interfacial tension of ILs are available in literature. In our previous studies,^{19,20,23} it was observed that σ of ILs containing the same cation is strongly influenced by the strength of electrostatic interactions between the anion and the cation. Referring to Tokuda et al.,³⁸ these interactions are affected by the Lewis basicity of the anion. The Lewis basicity was found to be high for anions having locally large negative charges with an asymmetric distribution and to be low for anions having symmetrically distributed low negative charges. Thus, a high Lewis basicity corresponds with a high interfacial tension. In addition, Law and Watson³⁹ found that the interfacial tension of ILs with the same cation increases with increasing molecular size of the anions being highly symmetrical such as $[\text{Cl}]^-$, $[\text{BF}_4]^-$, or $[\text{PF}_6]^-$. The reason for the lower interfacial tension of $[\text{EMIM}][\text{B}(\text{CN})_4]$ compared with $[\text{EMIM}][\text{N}(\text{CN})_2]$ is probably the strong charge delocalization¹¹ and thus low Lewis basicity of $[\text{B}(\text{CN})_4]^-$, confirming the explanations of Tokuda et al.³⁸ The same behavior seems to be the reason for the lower interfacial tension of $[\text{EMIM}][\text{B}(\text{CN})_4]$ compared to $[\text{EMIM}][\text{BF}_4]$,²³ an IL with a smaller and symmetrical anion. This observation is in disagreement with the conclusions of Law and Watson.³⁹ Furthermore, $[\text{EMIM}][\text{B}(\text{CN})_4]$ shows higher values than $[\text{EMIM}][\text{NTf}_2]$,¹⁹ possibly due to lower charge delocalization in the smaller $[\text{B}(\text{CN})_4]^-$ anion than in the large $[\text{NTf}_2]^-$ anion.

For the interfacial tension, a comparison of our data obtained from SLS with experimental data from Tong et al.¹⁶ can be drawn. They found significantly larger interfacial tensions compared with the SLS values, where the deviation is more pronounced for higher temperatures. The deviations are 8.1 % at 313.15 K and 13.8 % at 333.15 K. The authors report that a tensiometer based on the forced bubble method was used with a temperature uncertainty of ± 0.05 K and an experimental uncertainty in the interfacial tension values of ± 0.2 mN·m⁻¹.

Viscosity. The results for the dynamic viscosity from SLS at temperatures between (283.15 and 363.15) K at atmospheric pressure are shown in Table 5. Each data point represents the

Table 5. Dynamic Viscosity η of $[\text{EMIM}][\text{B}(\text{CN})_4]$ from $T = (283.15 \text{ to } 363.15)$ K at Atmospheric Pressure

T	η
K	mPa·s
283.15	37.06
288.15	27.75
293.15	21.79
303.15	14.65
313.15	10.09
323.15	7.61
333.15	5.77
343.15	4.67
353.15	3.70
363.15	3.16

average of six independent measurements with different moduli of the wave vectors q . The experimental data can well be represented in the form of a Vogel equation,

$$\eta_{\text{calc}} = \eta_0 \exp[B/(T - C)] \quad (7)$$

where T is the temperature in K, and $\eta_0 = 0.15660$ mPa·s, $B = 533.987$ K, and $C = 185.231$ K are the fit parameters found for

$[\text{EMIM}][\text{B}(\text{CN})_4]$. For the data correlation, the statistical weight of each data point has been assumed to be the same. The root-mean-square deviation of the viscosity data from the fit is 1.37 %. The relative deviation of the single data points from the fit is clearly smaller than the expanded uncertainty ($k = 2$) of less than ± 3 % for temperatures between (283.15 to 303.15) K and (343.15 and 363.15) K, and ± 6 % in the transition region for $T = (313.15 \text{ to } 333.15)$ K. Beside the entanglement between the molecules, the viscosity of ILs is generally governed by Coulomb forces, van der Waals (vdW) interactions, and hydrogen bonding. Bonhôte et al.⁴⁰ stated in their work that charge delocalization within the anion weakens intermolecular hydrogen bonding with the cation, leading to lower viscosities if not overcompensated by vdW interactions. These structure–property relationships were confirmed for the ILs in our previous works.^{19,20} In the $[\text{B}(\text{CN})_4]^-$ anion, the negative charge is uniformly delocalized over the four cyano groups tetrahedrally surrounding the boron cation.¹¹ In consequence, $[\text{B}(\text{CN})_4]^-$ is considered to be a relatively weakly coordinating anion.³⁰ In addition to this, the low viscosity of $[\text{EMIM}][\text{B}(\text{CN})_4]$ can also be attributed to the relatively low molecular weight of the anion as well as to the weak vdW interactions of the cation due to the short ethyl chain. Compared with previously studied ILs^{19,20} and other $[\text{EMIM}]$ -based ILs such as $[\text{EMIM}][\text{BF}_4]$ ^{15,41,42} and $[\text{EMIM}][(\text{FSO}_2)_2\text{N}]$,¹⁵ the investigated IL has the lowest viscosity, even lower than that of $[\text{EMIM}][\text{N}(\text{CN})_2]$,¹⁹ which is known as a very low-viscosity IL. The strong charge delocalization of the $[\text{B}(\text{CN})_4]^-$ anion seems to compensate for its larger molecular size compared with the $[\text{N}(\text{CN})_2]^-$ anion. The increase of vdW interactions from $[\text{EMIM}][\text{N}(\text{CN})_2]$ to $[\text{EMIM}][\text{B}(\text{CN})_4]$ is expected to be low. In addition, viscosity data for $[\text{EMIM}][\text{NTf}_2]$ ¹⁹ are higher compared to $[\text{EMIM}][\text{B}(\text{CN})_4]$. For the viscosity of $[\text{EMIM}][\text{B}(\text{CN})_4]$, four other very inconsistent data sources are available in the literature; see Figure 4. Mahurin et al.¹³ report a value of 17 mPa·s for a temperature of 298 K. The value deviates by -4.5 % from the correlation

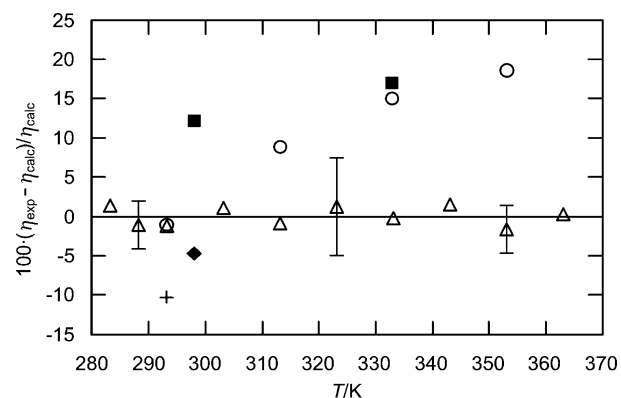


Figure 4. Deviation of experimental dynamic viscosities η of $[\text{EMIM}][\text{B}(\text{CN})_4]$ at atmospheric pressure for temperatures between (283.15 and 363.15) K from the correlation (—, eq 7): Δ , this work; \blacklozenge , Mahurin et al.;¹³ \blacksquare , Pitner and Ignatyev;¹⁵ \circ , Uerdingen;¹⁷ $+$, Welz-Biermann et al.¹⁸ Estimated expanded uncertainties ($k = 2$) of the present measurements are exemplarily shown as errors bars.

obtained in this work. The authors give no information on the instrument used, its uncertainty, or the water content of the investigated sample. The measurements of Pitner and Ignatyev¹⁵ deviate by 12.1 % at 298 K and 17.0 % at 333 K

from our correlation. The experiments were performed with an Anton Paar SVM 3000 viscosimeter according to the Stabinger principle. The measurement uncertainty for the data in the expanded temperature range is stated as $\pm 1\%$. The data set provided by Uerdingen¹⁷ was measured with the same instrument including the same uncertainty as performed by Pitner and Ignatyev.¹⁵ At 293.15 K, the datum is 1.1 % lower than the fit to our data, while increasing T leads to positive deviations of up to 18.6 % at 353.15 K. Here, the water content of the samples investigated by Uerdingen¹⁷ is stated as 4 ppm. Welz-Biermann et al.¹⁸ report for the viscosity of [EMIM]-[B(CN)₄] a value of 19.8 mPa·s at 293.15 K, without stating the method and uncertainty.

CONCLUSION

This work presents several thermophysical properties of the imidazolium-based IL [EMIM][B(CN)₄] in dependence on temperature at atmospheric pressure. The experimental data for the density, refractive index, self-diffusion coefficients, interfacial tension, and viscosity were discussed qualitatively in connection with other [EMIM]-based ILs. The results show that the thermophysical properties of [EMIM][B(CN)₄] are strongly influenced by the high charge delocalization in the anion and thus its weak interaction with the cation. The most remarkable characteristic of the IL is its very low viscosity which makes it attractive for different applications, in particular for its use in gas separation processes and electrolyte applications. In addition, a comparison with available literature for [EMIM][B(CN)₄] was drawn, yet at present only a scarce data situation can be found. The disagreements between different data sources may be attributed to an inconsistent sample purity and unspecified experimental conditions but also influenced by inconsistent experimental techniques as well as an inadequate estimation of their uncertainty.

AUTHOR INFORMATION

Corresponding Author

*E-mail: apf@aot.uni-erlangen.de. Tel.: +49 9131 85 29789. Fax: +49 9131 85 29901.

Funding

This work was supported by the German Research Foundation (Deutsche Forschungsgemeinschaft, DFG) by funding the Erlangen Graduate School in Advanced Optical Technologies (SAOT) within the German Excellence Initiative and via the DFG-SPP1191 priority program, grants FR 1709/9-1 and WA 1615/8-2.

Notes

The authors declare no competing financial interest.

REFERENCES

- (1) Smiglak, M.; Metlen, A.; Rogers, R. D. The Second Evolution of Ionic Liquids: From Solvents and Separations to Advanced Materials - Energetic Examples from the Ionic Liquid Cookbook. *Acc. Chem. Res.* **2007**, *40*, 1182–1192.
- (2) Chiappe, C.; Pieraccini, D. Ionic Liquids: Solvent Properties and Organic Reactivity. *J. Phys. Org. Chem.* **2005**, *18*, 275–297.
- (3) Balducci, A.; Soavi, F.; Mastragostino, M. The Use of Ionic Liquids as Solvent-Free Green Electrolytes for Hybrid Supercapacitors. *Appl. Phys. A: Mater. Sci. Process.* **2006**, *82*, 627–632.
- (4) Fukushima, T.; Aida, T. Ionic Liquids for Soft Functional Materials with Carbon Nanotubes. *Chem.—Eur. J.* **2007**, *13*, 5048–5058.
- (5) Schroer, K.; Tacha, E.; Lutz, S. Process Intensification for Substrate-Coupled Whole Cell Ketone Reduction by In Situ Acetone Removal. *Org. Process Res. Dev.* **2007**, *11*, 836–841.
- (6) Van Valkenburg, M. E.; Vaughn, R. L.; Williams, M.; Wilkes, J. S. Thermochemistry of Ionic Liquid Heat-Transfer Fluids. *Thermochim. Acta* **2005**, *425*, 181–188.
- (7) Wasserscheid, P.; Keim, W. Ionic Liquids - New “Solutions” for Transition Metal Catalysis. *Angew. Chem., Int. Ed.* **2000**, *39*, 3773–3789.
- (8) Wei, D.; Ivaska, A. Applications of Ionic Liquids in Electrochemical Sensors. *Anal. Chim. Acta* **2008**, *607*, 126–135.
- (9) Welton, T. Room-Temperature Ionic Liquids. Solvents for Synthesis and Catalysis. *Chem. Rev.* **1999**, *99*, 2071–2083.
- (10) Fröba, A. P. *Dynamic Light Scattering (DLS) for the Characterization of Working Fluids in Chemical and Energy Engineering*. Habilitation thesis, Friedrich-Alexander-Universität Erlangen-Nürnberg, Erlangen, 2009.
- (11) Kuang, D.; Wang, P.; Ito, S.; Zakeeruddin, S. M.; Grätzel, M. Stable Mesoscopic Dye-Sensitized Solar Cells Based on Tetracyanoborate Ionic Liquid Electrolyte. *J. Am. Chem. Soc.* **2006**, *128*, 7732–7733.
- (12) Kuang, D.; Klein, C.; Snaith, H. J.; Humphry-Baker, R.; Zakeeruddin, S. M.; Grätzel, M. A New Ion-Coordinating Ruthenium Sensitizer for Mesoscopic Dye-Sensitized Solar Cells. *Inorg. Chim. Acta* **2008**, *361*, 699–706.
- (13) Mahurin, S. M.; Lee, J. S.; Baker, G. A.; Luo, H.; Dai, S. Performance of Nitrile-Containing Anions in Task-Specific Ionic Liquids for Improved CO₂/N₂ Separation. *J. Membr. Sci.* **2010**, *353*, 177–183.
- (14) Ravichandar, B.; Sheng, D.; De-en, J. Understanding the High Solubility of CO₂ in an Ionic Liquid with the Tetracyanoborate Anion. *J. Phys. Chem. B* **2011**, *115*, 9789–9794.
- (15) Pitner, W. R.; Ignatyev, N. In *Ionic Liquids for Electrochemical Applications*, 214th Electrochemical Society Meeting, Honolulu, Hawaii, October, 12–17, 2008.
- (16) Tong, J.; Liu, Q.-S.; Kong, Y.-X.; Fang, D.-W.; Welz-Biermann, U.; Yang, J.-Z. Physicochemical Properties of an Ionic Liquid [C₂mim][B(CN)₄]. *J. Chem. Eng. Data* **2010**, *55*, 3693–3696.
- (17) Uerdingen, M. *Personal communication*, Sept 15, 2011.
- (18) Welz-Biermann, U.; Ignatyev, N.; Bernhardt, E.; Finze, M.; Willner, H. DE Patent WO/2004/072089, 26 August, 2004.
- (19) Fröba, A. P.; Kremer, H.; Leipertz, A. Density, Refractive Index, Interfacial Tension, and Viscosity of Ionic Liquids [EMIM][EtSO₄], [EMIM][NTf₂], [EMIM][N(CN)₂], and [OMA][NTf₂] in Dependence on Temperature at Atmospheric Pressure. *J. Phys. Chem. B* **2008**, *112*, 12420–12430.
- (20) Hasse, B.; Lehmann, J.; Assenbaum, D.; Wasserscheid, P.; Leipertz, A.; Fröba, A. P. Viscosity, Interfacial Tension, Density, and Refractive Index of Ionic Liquids [EMIM][MeSO₃], [EMIM][MeOHPO₂], [EMIM][OcSO₄], and [BBIM][NTf₂] in Dependence on Temperature at Atmospheric Pressure. *J. Chem. Eng. Data* **2009**, *54*, 2576–2583.
- (21) Fröba, A. P.; Leipertz, A. Accurate Determination of Liquid Viscosity and Surface Tension Using Surface Light Scattering (SLS): Toluene under Saturation Conditions between 260 and 380 K. *Int. J. Thermophys.* **2003**, *24*, 895–921.
- (22) Fröba, A. P.; Leipertz, A. Viscosity of Diisodecyl Phthalate by Surface Light Scattering (SLS). *J. Chem. Eng. Data* **2007**, *52*, 1803–1810.
- (23) Kolbeck, C.; Lehmann, J.; Lovelock, K. R. J.; Cremer, T.; Pappe, N.; Wasserscheid, P.; Fröba, A. P.; Maier, F.; Steinrück, H.-P. Density and Surface Tension of Ionic Liquids. *J. Phys. Chem. B* **2010**, *114*, 17025–17036.
- (24) Price, W. S. Pulsed-Field Gradient Nuclear Magnetic Resonance as a Tool for Studying Translational Diffusion: Part 1. Basic Theory. *Concepts Magn. Reson.* **1997**, *9*, 299–336.
- (25) Fröba, A. P. *Simultane Bestimmung von Viskosität und Oberflächenspannung transparenter Fluide mittels Oberflächenlichtstreuung*. Dr.-Ing. thesis, Friedrich-Alexander-Universität Erlangen-Nürnberg, Erlangen, 2002.

- (26) Langevin, D. *Light Scattering by Liquid Surfaces and Complementary Techniques*; Marcel Dekker: New York, 1992.
- (27) Levich, V. G. *Physicochemical Hydrodynamics*; Prentice Hall: Englewood Cliffs, 1962.
- (28) Lucassen-Reynders, E. H.; Lucassen, J. Properties of Capillary Waves. *Adv. Colloid Interface Sci.* **1969**, *2*, 347–395.
- (29) Fredlake, C. P.; Crosthwaite, J. M.; Hert, D. G.; Aki, S. N. V. K.; Brennecke, J. F. Thermophysical Properties of Imidazolium-Based Ionic Liquids. *J. Chem. Eng. Data* **2004**, *49*, 954–964.
- (30) Bernsdorf, A.; Brand, H.; Hellmann, R.; Köckerling, M.; Schulz, A.; Villinger, A.; Voss, K. Synthesis, Structure, and Bonding of Weakly Coordinating Anions Based on CN Adducts. *J. Am. Chem. Soc.* **2009**, *131*, 8958–8970.
- (31) Deetlefs, M.; Seddon, K. R.; Shara, M. Predicting Physical Properties of Ionic Liquids. *Phys. Chem. Chem. Phys.* **2006**, *8*, 642–649.
- (32) Brocos, P.; Piñeiro, Á.; Bravo, R.; Amigo, A. Refractive Indices, Molar Volumes and Molar Refractions of Binary Liquid Mixtures: Concepts and Correlations. *Phys. Chem. Chem. Phys.* **2003**, *5*, 550–557.
- (33) Tokuda, H.; Hayamizu, K.; Ishii, K.; Susan, M. A. B. H.; Watanabe, M. Physicochemical Properties and Structures of Room-Temperature Ionic Liquids. 2. Variation of Alkyl Chain Length in Imidazolium Cation. *J. Phys. Chem. B* **2005**, *109*, 6103–6110.
- (34) Noda, A.; Hayamizu, K.; Watanabe, M. Pulsed-Gradient Spin-Echo ^1H and ^{19}F NMR Ionic Diffusion Coefficient, Viscosity, and Ionic Conductivity of Non-Chloroaluminate Room-Temperature Ionic Liquids. *J. Phys. Chem. B* **2001**, *105*, 4603–4610.
- (35) Reid, R. C.; Prausnitz, J. M.; Poling, B. E. *The Properties of Gases and Liquids*; McGraw-Hill: New York, 1987.
- (36) MacLeod, D. B. On a Relation between Surface Tension and Density. *Trans. Faraday Soc.* **1923**, *19*, 38–41.
- (37) Sugden, S. The Variation of Surface Tension with Temperature and Some Related Functions. *J. Chem. Soc.* **1924**, *125*, 32–41.
- (38) Tokuda, H.; Tsuzuki, S.; Susan, M. A. B. H.; Hayamizu, K.; Watanabe, M. How Ionic are Room-Temperature Ionic Liquids? An Indicator of the Physicochemical Properties. *J. Phys. Chem. B* **2006**, *110*, 19593–19600.
- (39) Law, G.; Watson, P. R. Surface Tension Measurements of n-Alkylimidazolium Ionic Liquids. *Langmuir* **2001**, *17*, 6138–6141.
- (40) Bonhôte, P.; Dias, A. P.; Papageorgiou, N.; Kalyanasundaram, K.; Grätzel, M. Hydrophobic, Highly Conductive Ambient-Temperature Molten Salts. *Inorg. Chem.* **1996**, *35*, 1168–1178.
- (41) Nishida, T.; Tashiro, Y.; Yamamoto, M. Physical and Electrochemical Properties of 1-Alkyl-3-methylimidazolium Tetrafluoroborate for Electrolyte. *J. Fluorine Chem.* **2003**, *120*, 135–141.
- (42) Shirota, H.; Mandai, T.; Fukazawa, H.; Kato, T. Comparison between Dicationic and Monocationic Ionic Liquids: Liquid Density, Thermal Properties, Surface Tension, and Shear Viscosity. *J. Chem. Eng. Data* **2011**, *56*, 2453–2459.